

## MULTI-FIELD COUPLING DYNAMIC MODEL FOR PERMANENT-MAGNET SYNCHRONOUS MOTOR BASED ON FORWARD DESIGN

Dong Wei<sup>1</sup>, Hongwen He<sup>1\*</sup>, Jianfei Cao<sup>1</sup>, Yunfei Bai<sup>1</sup>

<sup>1</sup> National engineering laboratory for electric vehicles, Beijing Institute of Technology, Beijing 100081, China

### ABSTRACT

PMSM is a heated research field in terms of the HEVs. In order to increase the efficiency and output characteristics of the PMSM, the design and modeling method which can design the PMSM according to its performance requirements is necessary. In this paper, a new modeling method for multi-field coupling dynamic analysis for PMSMs based on forward design theory is proposed and verified. In particular, given some performance parameters, stator and rotor structural parameters can be decided by electromagnetic load prefetching algorithm and maximum torque method. Besides, the mathematical model of the PMSM power losses achieves an evaluation of the motor output performance effectively. Simulation results compared with the PMSM experimental data show the proposed approach is valid.

**Keywords:** Permanent-magnet synchronous motor (PMSM), multi-field coupling, dynamic model, forward design.

### NONMENCLATURE

#### Abbreviations

|      |                                    |
|------|------------------------------------|
| AC   | Alternating current                |
| DC   | Direct current                     |
| HEV  | Hybrid Electric Vehicle            |
| PMSM | Permanent-magnet synchronous motor |

#### Symbols

|            |                                  |
|------------|----------------------------------|
| $I, I_N$   | Actual and rated current (A)     |
| $\rho$     | Air density (kg/m <sup>3</sup> ) |
| $B_\delta$ | Air gap flux density (T)         |
| $\delta$   | Air gap length (cm)              |

|                               |   |
|-------------------------------|---|
| $L_{ef}, L_2$                 | Armature calculation and rotor axial lengths (cm)                   |
| $L_{av}$                      | Average half turn length of coil (cm)                               |
| $P', P_N$                     | Calculation and rated powers (kW)                                   |
| $\alpha_i$                    | Calculation polar arc coefficient                                   |
| $B_r$                         | Calculation residual magnetic density (T)                           |
| $P_{Cu}, P_{Fe}, P_s, P_{fw}$ | Copper, iron, stray and rotor wind losses (kW)                      |
| $A_m$                         | Cross-sectional area of providing each pole flux (cm <sup>2</sup> ) |
| $R_{DC}$                      | DC resistance of each phase in the stator winding ( $\Omega$ )      |
| $B$                           | Flux density amplitude (T)  |
| $C_f$                         | Friction coefficient  |
| $K_h, K_f$                    | Hysteresis and classical loss constants                             |
| $T_{max}, T_e$                | Maximum and rated torques (Nm)                                      |
| $\omega_m, \omega_e$          | Mechanical and electrical angular velocities (rad/s)                |
| $f$                           | Motor frequency (Hz)  |
| $\sigma_0$                    | No-load leakage coefficient   |
| $a_1$                         | Number of parallel branches   |
| $p$                           | Number of pole pairs  |
| $P_L$                         | Overall power loss (kW)   |
| $b'_{m0}$                     | Permanent magnet no-load operating point assumed value              |
| $A$                           | Power load (A/cm)   |
| $Re_\delta, Re_a$             | Radial and tangential Reynolds numbers                              |
| $\eta_N$                      | Rated efficiency  |
| $\cos \varphi_N$              | Rated power factor  |
| $n_N$                         | Rated speed (r/min)   |
| $p_{SN}^*$                    | Ratio of stray loss to rated power at rated power                   |
| $\mu$                         | Relative permeability of rotor                                      |

|                        |  |
|------------------------|--|
|                        | material   |
| $\rho_{Cu}, \rho_{15}$ | Resistivity of copper at a given temperature and 15 ° C (kg/m <sup>3</sup> ) |
| $R_2$                  | Rotor radius (cm)  |
| $A_{Cu}$               | Sectional area of wire (cm <sup>2</sup> )                                    |
| $D_{i1}$               | Stator inner diameter (cm)   |
| $\beta$                | Steinmetz constant   |
| $\alpha$               | Temperature coefficient of conductor resistance (/°C)                        |
| $N_1$                  | Turn in series for each phase winding  |
| $K_B, K_E$             | Waveform and Potential coefficient   |
| $K_{dp}$               | Winding factor   |

## 1. INTRODUCTION

With the development of society and technology, the number of vehicles in the world is growing rapidly, followed by environment pollution and energy shortage [1]. HEVs have become a suitable scheme for the green energy vehicles because of having the advantages of low power consumption and long driving distance [2].

The driving motor which concerns the performance of the vehicle is the core component of the power system in the HEV. The PMSM has the advantages of small size, light weight, high efficiency, etc., making the PMSM the most competitive driving motor in HEV [3].

To improve the PMSM efficiency and output characteristics, it is necessary to make multi-field coupling analysis of the PMSM. Based on multi-field coupling theory, the modeling of a PMSM could be described and machine behaviors in terms of thermal, electromagnetic, and mechanical characteristics are predicted [4]. With the optimal design of a PMSM, a field-circuit coupled optimal design method would be presented under the comprehensive selection of variable parameters, objective functions and constraint conditions [5]. However, in recent modeling approaches, a specific motor, as a research object, was analyzed or optimized. To be specific, no corresponding motor is designed for certain working conditions and analyzed in the multi-field coupling model. Hence, the above problems limit the performance of the PMSM under different working conditions.

The purpose of this paper is to propose a new modeling approach for multi-field coupling dynamic analysis for the PMSM based on forward design theory. Electromagnetic load prefetching algorithm and maximum torque method are implemented to determine PMSM size parameters firstly. After that, the

mathematical model of the PMSM power losses is established based on the multi-field coupling theory, and the various losses during the operation of the motor are analyzed to provide a theoretical basis for the modeling of the motor system. In addition, a PMSM simulation model is built for multi-field coupling dynamic analysis. The proposed multi-field coupling dynamic technology is compared with the PMSM measured data in term of motor efficiency to demonstrate its effectiveness finally.

## 2. PMSM STRUCTURE PARAMETER DESIGN

In the PMSM forward design, Determining the stator and rotor structural parameters of the motor based on performance requirements previously proposed is an important part. In this process, electromagnetic load prefetching algorithm and maximum torque method play an important role. After selecting some structure parameters by experience, the main structure parameters of a PMSM can be obtained from  $D_{i1}$ , determined by electromagnetic load prefetching algorithm and  $L_{ef}$ , determined by maximum torque method.

### 2.1 Electromagnetic load prefetching algorithm

In order to meet the space constraints of the vehicle layout and the design requirements of the driving motor for lightweight, high power density and high torque density, the stator inner diameter of the PMSM cannot directly draw on that of the existing asynchronous motor. As  $P_N$ ,  $n_N$ , and  $p$  of the PMSM are known in advance and other parameters which vary in a small range could be based on experience.,  $D_{i1}$  of the PMSM can be calculated by:

$$D_{i1} = \frac{6.1 \times 10^7 P_N \sigma_0 \pi K_E}{2p K_B K_{dp} A b_{m0}^2 B_r A_m \eta_N \cos \varphi_N} \quad (1)$$

### 2.2 Maximum torque method

Likewise, the main dimensions of PMSM are related to the maximum torque required. Because  $D_{i1}$  has been gained by the electromagnetic load prefetching algorithm, in turn,  $L_{ef}$  is calculated as:

$$L_{ef} = \frac{4T_{max}}{\sqrt{2\pi} B_{\delta 1} D_{i1}^2} \times 10^4 \quad (2)$$

## 3. MATHEMATICAL MODEL OF PMSM POWER LOSSES

The power losses in a PMSM are mainly composed of copper loss, iron loss, stray loss and mechanical loss, which reflect the intercoupling of electric, magnetic,

thermal and mechanical fields. Therefore, the equation of the mathematical model of  $P_L$  is:

$$P_L = P_{Cu} + P_{Fe} + P_S + P_{fw} \quad (3)$$

### 3.1 Copper loss

The temperature of the winding affects the value of the copper loss resistance. In the normal temperature range,  $R_{DC}$  is:

$$R_{DC} = \rho_{Cu} \frac{2N_1 L_{av}}{a_1 A_{Cu}} \quad (4)$$

where

$$\rho_{Cu} = \rho_{15} [1 + \alpha(T - 15)] \quad (5)$$

When an AC current flows through the wire, the sectional area of the wire would be reduced due to the skin effect, so that the AC resistance of the winding is greater than the DC resistance. For the stator winding wound with cylindrical wire, the calculation of copper loss can ignore the skin effect when a low frequency current is applied. Thus,  $P_{Cu}$  is expressed as:

$$P_{Cu} = mI^2 R_{DC} \quad (6)$$

### 3.2 Iron loss

In the current studies, a classical iron loss model is the Bertotti loss separation model. In this model, the iron loss is divided into three parts: hysteresis loss, excess loss and classical loss. Since the excess loss is relatively small compared to the hysteresis loss and the classical loss, the excess loss can be ignored in the iron loss calculation. Therefore,  $P_{Fe}$  is calculated by the following formula:

$$P_{Fe} = K_h f B^\beta + K_f f^2 B^2 \quad (7)$$

### 3.3 Stray loss

Stray loss is generated in the core by the high harmonics of the magnetic field and the high harmonics caused by the cogging, and there are stray losses in the stator, air gap and cogging. Stray loss is difficult to express with mathematical models. Besides, the calculation is too complicated to obtain accurate results. So  $P_S$  can be roughly calculated by the following empirical formula:

$$P_S = \left(\frac{I}{I_N}\right)^2 p_{SN}^* P_N \quad (8)$$

### 3.4 Mechanical loss

The mechanical loss of a PMSM is mainly comprised of bearing friction loss and wind loss between the rotor and the air. In most cases, the mechanical loss is based on simple empirical formulas or existing motor experimental data. And as for the PMSM of HEVs, deep groove ball bearings which cause less friction are

employed. Hence, in this model, the bearing friction loss could be neglected. While  $P_{fw}$  is:

$$P_{fw} = C_f \rho \pi \omega_m^3 R_2^4 L_2 \quad (9)$$

where

$$C_f = \frac{0.0152}{Re_\delta^{0.24}} \left[1 + \left(\frac{8}{7}\right)^2 \left(\frac{4R_a}{Re_\delta}\right)^2\right]^{0.38} \quad (10)$$

$$Re_\delta = \frac{\rho \omega_m R_2 \delta}{\mu} \quad (11)$$

$$Re_a = \frac{\rho v_a 2\delta}{\mu} \quad (12)$$

## 4. DYNAMIC SIMULATION MODEL

Along with the mathematical model of the PMSM power losses which have been described, a multi-field coupling dynamic simulation model is built in MATLAB/Simulink. In this model, the intercoupling of electric, magnetic, thermal and mechanical fields is considered from the perspective of PMSM power losses. Fig 1 shows the structure of the PMSM forward design that includes the dynamic simulation model.

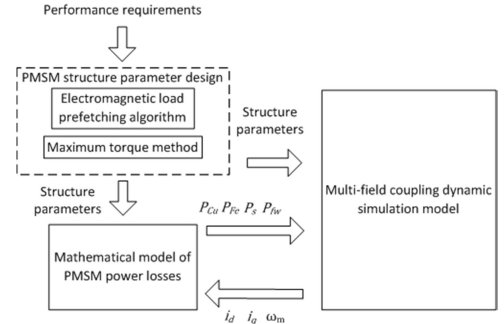


Fig 1 PMSM forward design structure

## 5. RESULT

In order to verify the feasibility of this multi-field coupling dynamic technology, a PMSM for the HEVs is selected as an example of this method. The performance requirements of the PMSM are listed in Table 1.

Table 1

Performance parameters of the PMSM

| Parameters           | Values  |
|----------------------|---------|
| DC power voltages    | 657V    |
| Rated torque         | 400Nm   |
| Maximum torque       | 900Nm   |
| Rated speed          | 2000rpm |
| Number of pole pairs | 6       |

At first,  $D_{i1}$  (233mm) and  $L_{ef}$  (304mm) are gained through electromagnetic load prefetching algorithm and maximum torque method. Then, these PMSM structure parameters are put into the mathematical model of the PMSM power losses to obtain the multi-field coupling dynamic simulation model. Besides, the model is asked for operating at

different feasible working points to gain the corresponding efficiency values. The three-dimensional images of the experimental data and simulation results about PMSM efficiency are displayed in Fig 2. The above two figures show the simulation results can reflect the overall trend of PMSM efficiency.

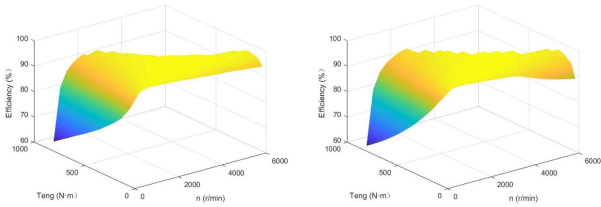


Fig 2 The experimental data and simulation results about PMSM efficiency

Apart from that, according to the experimental data, the error analysis of the above simulation results in Fig 3 demonstrates that when the motor operating point is in the areas of low speed low torque and high speed low torque, the errors of simulation results are a little large, reaching 5% and -5% respectively. While, the errors can reach about 1% in most other areas.

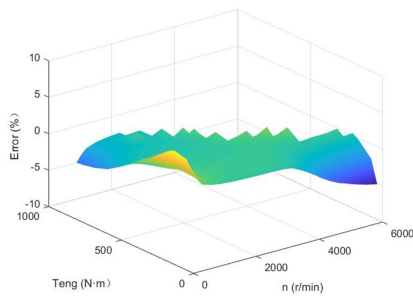


Fig 3 Three-dimensional error distribution map of the simulation results

Table 2  
Model simulation errors at specific operating points

| PMSM working points | simulation results (%) | experimental data (%) | errors (%) |
|---------------------|------------------------|-----------------------|------------|
| 150rpm, 250.92Nm    | 84.05                  | 80.85                 | 3.96       |
| 750rpm, 627.31Nm    | 91.31                  | 91.54                 | -0.25      |
| 1500rpm, 836.41Nm   | 93.99                  | 94.14                 | -0.16      |
| 1800rpm, 710.95Nm   | 95.61                  | 95.62                 | 0.01       |
| 2250rpm, 627.31Nm   | 96.78                  | 96.46                 | 0.33       |
| 2700rpm, 543.67Nm   | 97.51                  | 96.60                 | 0.94       |
| 3000rpm, 418.21Nm   | 98.04                  | 97.82                 | 0.22       |
| 4200rpm, 334.56Nm   | 97.83                  | 97.24                 | 0.61       |
| 5250rpm, 209.10Nm   | 97.19                  | 97.06                 | 0.13       |
| 6000rpm, 83.64Nm    | 93.89                  | 95.87                 | -2.07      |
| Average error (%)   |                        |                       | 0.87       |

Finally, as shown in Table 2, some model results and experimental data of the PMSM efficiency values in the specific working points are randomly selected from Fig 2 within the operational range. We can see the errors

corresponding to these values are all less than 4% and the average error is even 0.87%. These results mean the multi-field coupling dynamic technology is effective.

## 6. CONCLUSIONS

In this paper, a novel modeling approach for the multi-field coupling dynamic analysis for the PMSM is proposed to realize the forward design of the motor according to performance requirements. This method can design a PMSM according to performance requirements, avoiding the problem of many power surplus and low efficiency brought by high-power motors. In addition, the PMSM design flow from design to simulation analysis proposed in this paper can effectively shorten the design cycle of the motor, thus saving cost. Compared with the experimental data about the PMSM efficiency, the errors of the efficiency model results are small. We can say simulation results demonstrate the effectiveness of the multi-field coupling dynamic model for the PMSM of HEVs based on forward design.

## ACKNOWLEDGEMENT

This project is supported by National Key R&D Program of China (Grand No.2018YFB0105900) in part, and the National Natural Science Foundation of China (Grand No.51675042) in Part.

## REFERENCE

- [1] Wu J , He H , Peng J , et al. Continuous reinforcement learning of energy management with deep Q network for a power split hybrid electric bus. *Applied Energy* 2018; 222:799-811.
- [2] Moreno J, Ortuzar M E. Energy-management system for a hybrid electric vehicle, using ultracapacitors and neural networks. *IEEE Transactions on Industrial Electronics*, 2006; 53(2):614-623.
- [3] Park J S , Nam K . Dual Inverter Strategy for High Speed Operation of HEV Permanent Magnet Synchronous Motor. In: *Industry Applications Conference, IEEE; 2006.*
- [4] Chen Y , Chen W , Zhou J , et al. Multi-field coupled analysis of a permanent magnet synchronous motor: Application to high speed rail traction. In: *International Conference on Ecological Vehicles and Renewable Energies (EVER). IEEE;2016.*
- [5] Yaojing F , Shoudao H , Kai Y , et al. Research on optimal design of permanent magnet synchronous motors based on field-circuit coupled method. In: *International Conference on Electrical Machines & Systems. IEEE;2014.*